Electronic Supplementary Material (ESI) for Sustainable Energy & Fuels.

Supplementary Information

Transforming waste cigarette filters into 3D carbon scaffolds for form-stable and energy conversion phase change materials

Malik Muhammad Umair,[a] Yuang Zhang,[a] Shufen Zhang,[a] Xin Jin [b] and Bingtao Tang [*ab]

[a] State Key Laboratory of Fine Chemicals, Dalian University of Technology, Dalian 116024, PR China.

[b] Eco-chemical Engineering Cooperative Innovation Center of Shandong, Qingdao University of Science and Technology, Qingdao 266042, PR China.

[†] Email: tangbt@dlut.edu.cn

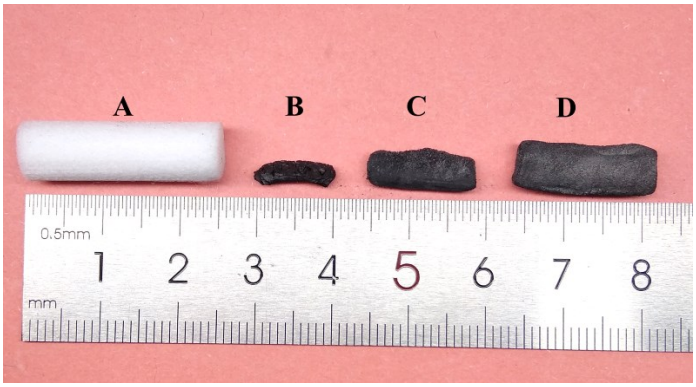

Fig. S1. Photograph of samples (A) CF, (B) carbonised GO (1 mg mL^{-1})@CF, (C) carbonised GO (5 mg mL^{-1})@CF, and (D) carbonised GO (10 mg mL^{-1})@CF.

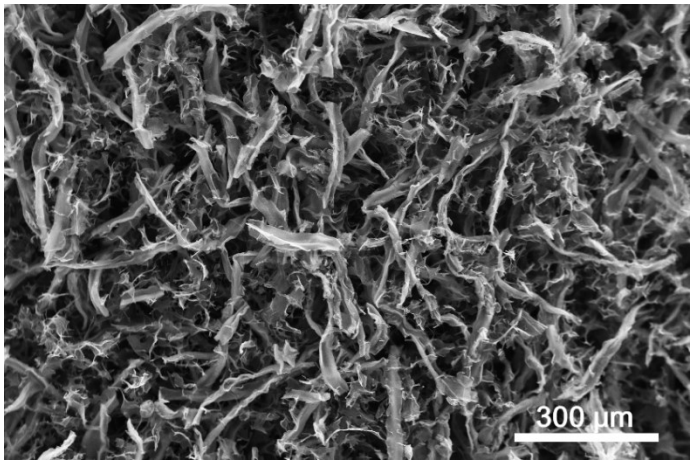

Fig. S2. SEM image of GPC scaffold.

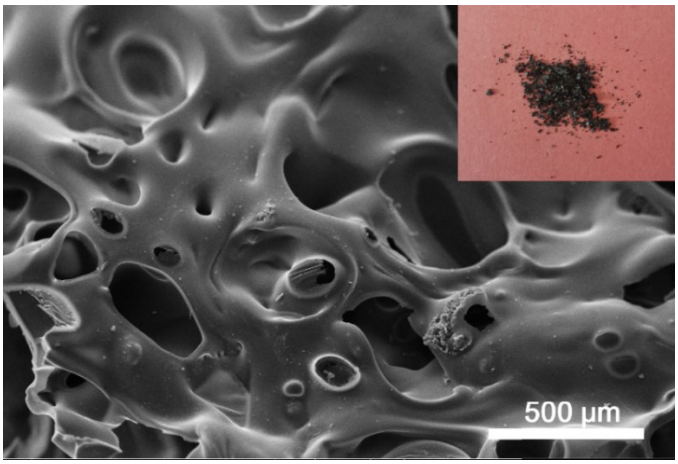

Fig. S3. SEM image of carbonised CF with the inset of digital photograph.

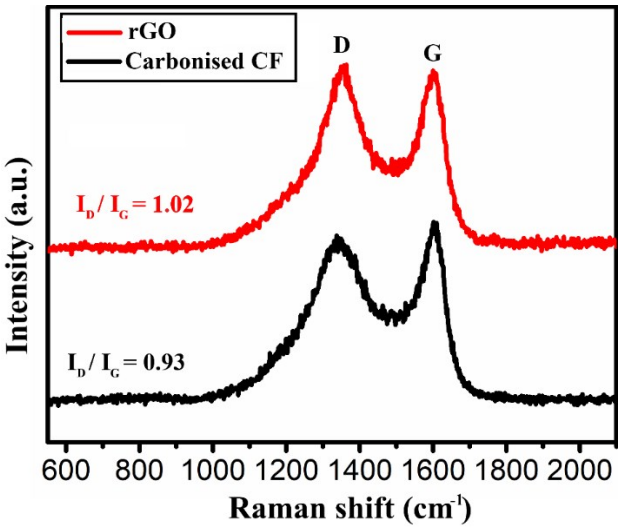

Fig. S4. Raman spectra of rGO and carbonised CF.

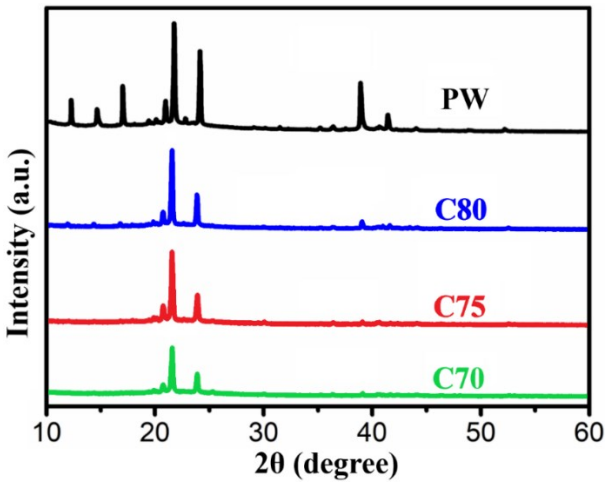

Fig. S5. XRD patterns of PW and PCM composites.

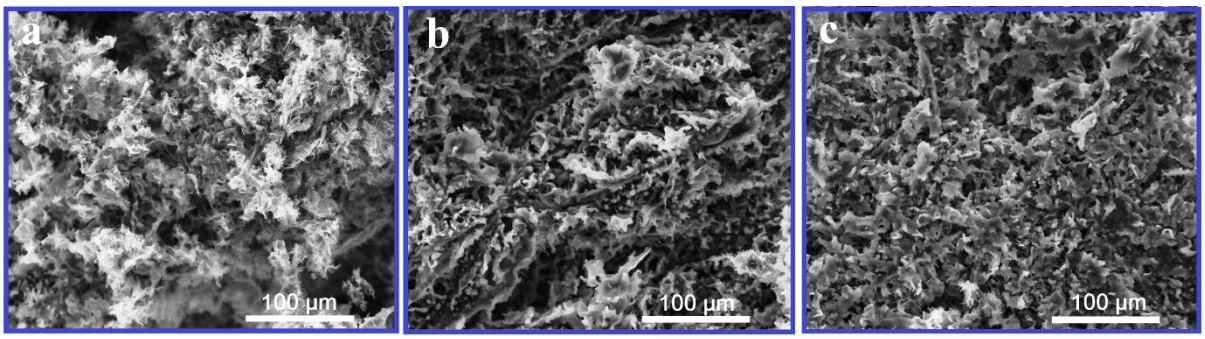

Fig. S6. SEM images of (a) C70, (b) C75 and (c) C80.

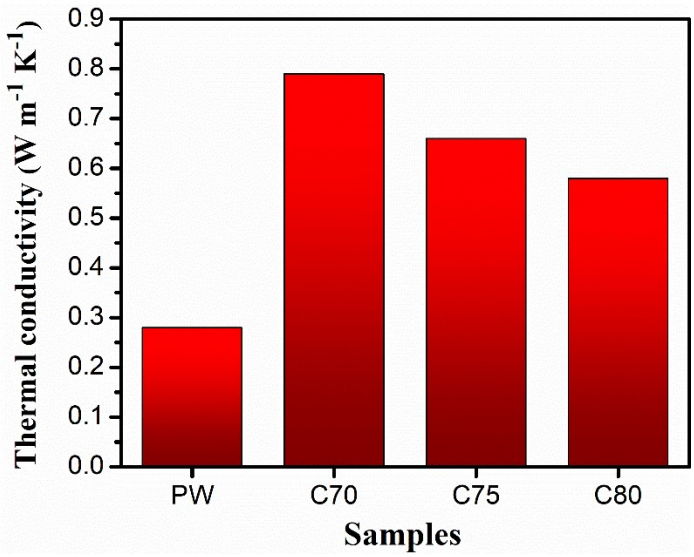

Fig. S7. Thermal conductivity of pure PW and PCM composites.

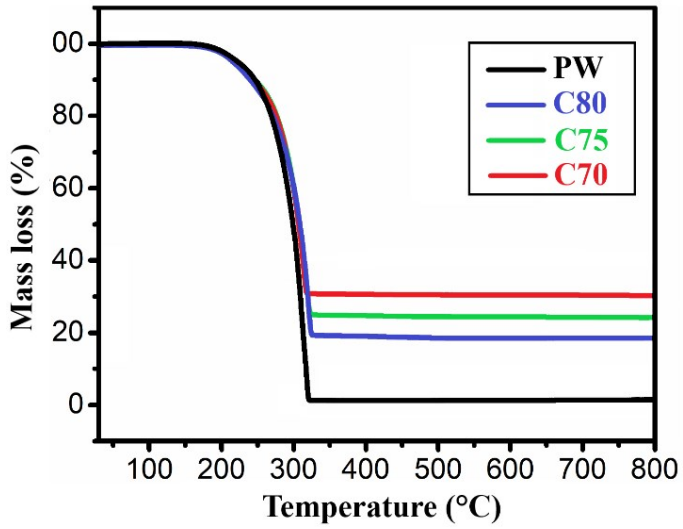

Fig. S8. TGA curves of PW and PCM composites.

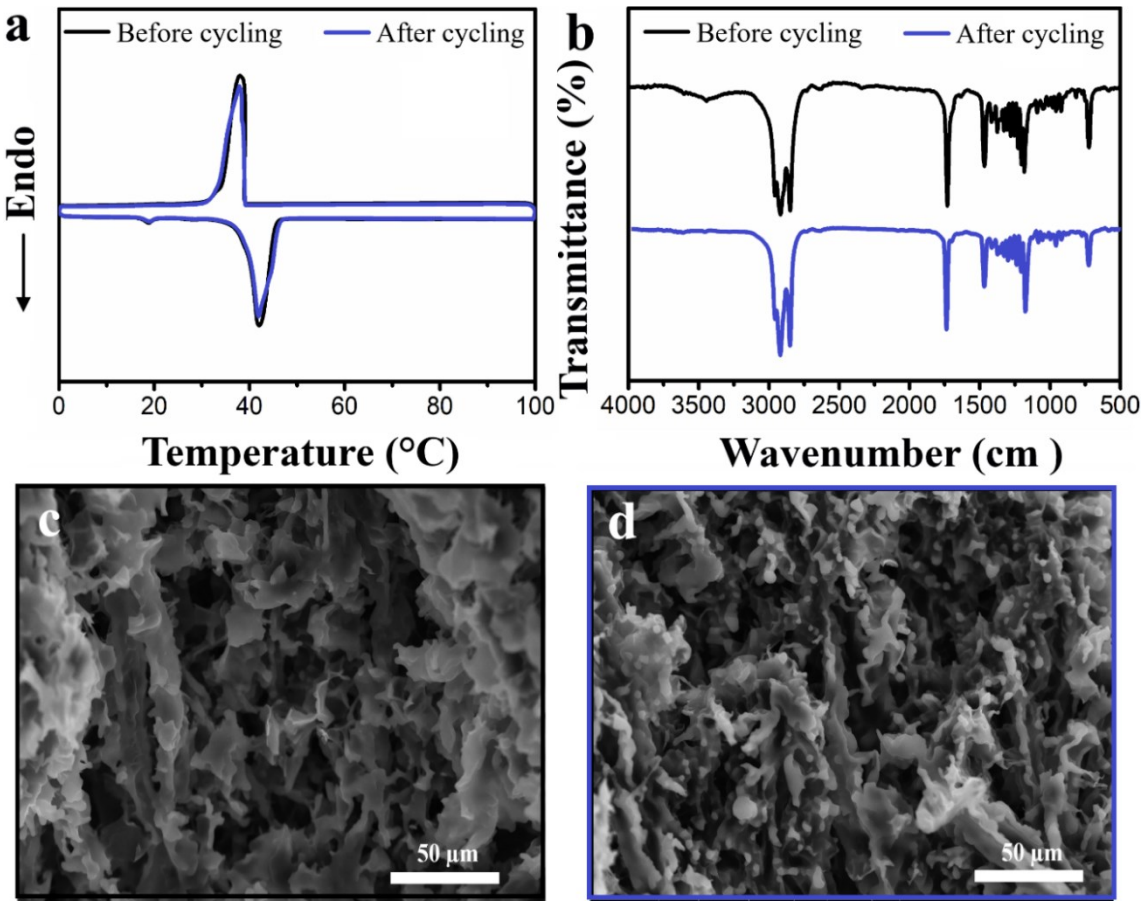

Fig. S9. DSC curves (a) and FTIR spectra (b) of C80 composite obtained before and after 200 heating-cooling cycles. SEM images of C80 composite before (c) and after (d) the cycling test.

Table S1. Thermal properties of PW and PCM composites

Samples	T_M (°C)	ΔH_M (J g^{-1})	ΔH^{Th} (J g^{-1})	T_C (°C)	ΔH_C (J g^{-1})
PW	40.47	196.1	-	39.79	206.8
C70	40.2	138.7	137.3	38.89	143.6
C75	40.17	149.5	147.1	37.2	154.4
C80	39.53	157	156.9	36.9	162.7

Table S2. Electrothermal storage efficiencies of various electro-driven PCMs

PCM composites	PCM content (%)	Efficiency (%)	References
CNTS-PW	87	52.5	S1
MF/rGO/GNP-PW	95	62.5	S2
Graphene aerogel-PW	94	85.4	S3
CNTs/GO-PEG	85	66.3	S4
Graphite foam-PU	82	80	S5
Carbon foam-PW	86	73	S6
CNTS-PU	90	94	S7
GPC-PW	80	88.7	This work

(S1) Aftab, W.; Mahmood, A.; Guo, W.; Yousaf, M.; Tabassum, H.; Huang, X.; Liang, Z.; Cao, A.; Zou, R. Polyurethane-based flexible and conductive phase change composites for energy conversion and storage. *Energy Storage Mater.* 2019, *20*, 401–409.

(S2) Chen, L.; Zou, R.; Xia, W.; Liu, Z.; Shang, Y.; Zhu, J.; Wang, Y.; Lin, J.; Xia, D.; Cao, A. Electro- and photodriven phase change composites based on wax-infiltrated carbon nanotube sponges. *ACS Nano* 2012, *6* (12), 10884–10892.

(S3) Xue, F.; Lu, Y.; Qi, X.; Yang, J.; Wang, Y. Melamine foam-templated graphene nanoplatelet framework toward phase change materials with multiple energy conversion abilities. *Chem. Eng. J.* 2019, *365*, 20–29.

(S4) Li, G.; Zhang, X.; Wang, J.; Fang, J. From anisotropic graphene aerogels to electron- and photo-driven phase change composites. *J. Mater. Chem. A* 2016, *4* (43), 17042–17049.

(S5) Guo, X.; Liu, C.; Li, N.; Zhang, S.; Wang, Z. Electrothermal conversion phase change composites: the case of polyethylene glycol infiltrated graphene oxide/carbon nanotube networks. *Ind. Eng. Chem. Res.* 2018, *57* (46), 15697–15702.

(S6) Chen, R.; Yao, R.; Xia, W.; Zou, R. Electro/photo to heat conversion system based on polyurethane embedded graphite foam. *Appl. Energy* 2015, *152*, 183–188.

(S7) Li, Y.; Samad, Y. A.; Polychronopoulou, K.; Alhassan, S. M.; Liao, K. From biomass to high performance solar–thermal and electric–thermal energy conversion and storage materials. *J. Mater. Chem. A* 2014, *2* (21), 7759–7765.